Supporting Information

Dual-Potential Electrochemiluminescence Ratiometric Approach Based on Graphene Quantum Dots and Luminol for Highly Sensitive Detection of Protein Kinase Activity

Hui-Fang Zhao, Ru-Ping Liang, Jing-Wu Wang, and Jian-Ding Qiu*

Department of Chemistry, Nanchang University, Nanchang 330031, China

* Corresponding author. Tel/Fax: +86 791 83969518. *E-mail address:* jdqiu@ncu.edu.cn (J.D. Qiu)

Materials and Reagents. Graphite powder (99.8%, 325 mesh) was provided by Alfa Aesar. Protein kinase A (PKA, catalytic subunit from recombinant E. coli strain) was obtained from New England Biolabs (UK). Cysteine-terminated peptide (H-CGGGGLSARRL-OH) was purchased from GL Biochem (Shanghai, China). Chitosan (CS), N-ethyl-N'-(3-dimethylaminopropyl)carbodiimide (EDC), N-hydroxysuccinimide (NHS), adenosine 5′-[γ-thio] triphosphate tetra-lithium salt (ATP-s), 4,4′,5,5′,6,6′-hexahydroxydiphenic acid 2,6,2′,6′-dilactone (ellagic acid), hydrogen tetrachloroaurate ($HAuCl_4 \cdot 4H_2O$), and luminol were purchased from Sigma-Aldrich (USA). A 1.0×10^{-3} M stock solution of luminol was prepared by dissolving luminol in 0.1 mol/L NaOH solution. Dulbecco's Modified Eagle Medium (DMEM) and fetal bovine serum (FBS) were purchased from Thermo Scientific HyClone (MA, USA). Other chemicals were of analytical grade and were used as received without further purification. All solutions were prepared using ultrapure water (18.3 MΩ cm) from a Millipore Milli-Q system. Human serum samples were provided by Jiangxi Provincial People's Hospital.

Apparatus. Transmission electron microscopy (TEM) images were obtained using a JEOL Ltd. JEM-2010 transmission electron microscopy. Fourier transform infrared (FTIR) spectra were obtained on a Bruker Tensor 27 spectrometer. The photoluminescence (PL) spectra were measured on a Hitachi F-7000 fluorescence spectrophotometer (Tokyo, Japan). UV-vis spectra were collected on an UV-2450 spectrophotometer (Shimadzu, Japan). Electrochemical impedance spectroscopy (EIS) was carried out on an Autolab PGSTAT30 electrochemical workstation (Eco Chemie, Netherlands). Impedance measurements were performed by applying an ac voltage of 5 mV amplitude in the 0.01 Hz to 10^6 Hz frequency range in a 5 mM $K_3[Fe(CN)_6]/K_4[Fe(CN)_6]$ redox probe solution containing 0.1 M KCl. The cyclic voltammograms (CVs) were recorded in voltage sweeps between −0.1 V and +0.6 V with a scan rate of 100 mV/s in a 5 mM $K_3[Fe(CN)_6]/K_4[Fe(CN)_6]$ redox probe solution containing 0.1 M KCl. The ECL measurements were carried out on an MPI-B multifunctional electrochemical analytical system (Xi'an Remex Analytical Instrument Ltd. Co., China). The system provided an electrochemical potentiostat for the ECL detection, a multifunction chemiluminescence detector and a multichannel data collection analyzer to connect with the other parts. Output ECL intensity was amplified and recorded in a computer using the MPI-B software. ECL intensities were measured through the bottom of the cell with a photomultiplier tube (PMT) window, and all of them were enclosed in a light-tight box. The PMT was operated in current mode, unless noted, otherwise the PMT was biased at 800 V. The ECL cell was composed of a modified glassy carbon working electrode (φ = 3 mm), a saturated calomel reference electrode (SCE), and a Pt wire counter electrode.

Synthesis of Graphene Oxide Sheets and GQDs. Graphene oxide (GO) was synthesized

from natural graphite powder by a modified Hummers and Offeman method.[1] In brief, 0.5 g of graphite powder, 0.5 g of $NaNO_3$, and 23 mL of H_2SO_4 were added to a three-neck flask with stirring in an ice bath. Next, 3 g of $KMnO_4$ was slowly added to ensure that the temperature remained below 20 °C during the process. After the contents were mixed together, the flask was transferred to a 35 ± 5 °C water bath for 1 h with stirring, and then a brown paste was obtained. Then, 40 mL of ultrapure water was added, and the solution was stirred for 30 min. Another 100 mL of ultrapure water was added, and then the dropwise addition of 3 mL of H_2O_2 (30 wt %) made the color of the solution change to bright yellow. The warm GO solution was filtered and washed with ultrapure water until the pH was 7.0. The precipitates were dried in a vacuum drying oven at 50 °C.

The GQDs were prepared from graphene sheets (GSs) by a hydrothermal approach as described in the literature.[2] GSs were produced by heating the dried GO to 200 °C with a heating rate of 5 °C/min and then maintained at 200 °C for 2 h in a tube furnace under a nitrogen atmosphere. GSs (0.05 g) were oxidized with concentrated H_2SO_4 and HNO_3 (volume ratio 1:3) for 17 h under mild ultrasonication. The solution was diluted with distilled water (250 mL), and then filtered through a 0.22 mm microporous membrane to remove the acids. The filter cake was collected and redispersed in distilled water (40 mL). The pH was adjusted to 8 with NaOH. The oxidized GS suspension was placed into a poly (tetrafluoroethylene) (Teflon)-lined autoclave and heated at 200 °C for 12 h. After cooling to room temperature, the resulting solution was filtered through a 0.22 μm microporous membrane to remove the large tracts of GSs. The brown filtrate was the GQDs solution. The resulting GQDs was taken for further carboxylation according to a method reported previously.[3] Briefly, 0.05 g NaOH and 0.1 g $ClCH_2COONa$ were added into 20 mL GQDs

solution, followed by bath sonication for 3 h to covert hydroxyl groups into carboxyl groups. And the resultant product was neutralized with HCl, and purified by repeated centrifugation at 125,000 rpm for 10 min and rinsing with distilled water. The sediment was re-dispersed in 20 mL phosphate buffer solution (PBS) (pH 7.4) to obtain the carboxylated GQDs solution.

Preparation of Gold Nanoparticles. Au NPs were prepared as reported previously.[4] In brief, 50 mL of 0.05 g/L $HAuCl_4 \cdot 4H_2O$ solution was added into a 100 mL round flask, and was heated to boiling. Then, 5 mL of 1% sodium citrate solution was added rapidly under vigorous stirring. The solution was maintained at the boiling state for 10 min, during which time the color changed from yellow to deep wine red. A stable and monodispersed Au NPs colloidal solution was obtained and stored at 4 °C.

Assembly and Phosphorylation of Peptides on Glassy Carbon Electrode. The glassy carbon electrode (GCE) was polished carefully with 1.0, 0.3, and 0.05 μm α-Al_2O_3 powder on fine abrasive paper and then thoroughly rinsed with ethanol and water. After the electrode was rinsed thoroughly with ultrapure water and allowed to dry with N_2 at room temperature, 10 μL CS solution (0.5% w/w) was dropped on the GCE surface and dried in air. The resulting CS/GCE was then immersed in a solution containing 0.1 mg/mL carboxylated GQDs and 5 mM EDC for 5 h at room temperature to obtain GQDs/CS/GCE. After rinsing with 0.01 M pH 7.4 PBS, the electrode was dipped into a solution containing 5 mM EDC, 8 mM NHS, and 100 μM peptide at room temperature in darkness for 8 h to yield peptide/GQDs/CS/GCE. PKA-catalyzed peptide phosphorylation was performed by incubating the peptide/GQDs/CS/GCE into an assay buffer solution (20 mM Tris-HCl and 20 mM $MgCl_2$, pH 7.4) containing a desired amount of PKA and adenosine 5′-[γ-thio] triphosphate (ATP-s)

at 30 °C for 1 h. The phosphorylated peptide/GQDs/CS/GCE was obtained (Scheme 1). For PKA inhibitor assay, the procedures were similar as above, except for a desired concentrations of inhibitors were added in the assay buffer solutions.

Preparation of Cell Lysates. MCF-7 Cells (5×10^6 cells) were cultured in DMEM medium supplemented with 10% FBS at 37 °C in a humid atmosphere containing 5% CO_2. Subsequently, cells were treated with 1 mL of lysis buffer for 30 min at 4 °C. After the above step, the cell lysate was then centrifuged at 12000 rpm for 20 min and the resulting supernatants were stored at −20 °C before use. The analysis of PKA activity in complex biological samples were performed by diluting the cell lysates into desired volumes of PKA assay buffer (20 mM Tris-HCl, 20 mM $MgCl_2$, pH 7.4, 50 μM ATP-s).

ECL Characterization and Kinase Activity Detection. The phosphorylated peptide/GQDs/CS/GCE was immersed into Au NPs solution at room temperature for 1 h to adsorb Au NPs onto the phosphorylated peptide modified electrode surface through the Au-S bond. After washing to remove the nonspecific Au NPs, the resulting electrode was characterized by an ECL technique in a 0.1 M pH 7.4 PBS buffer solution containing 1.0 mM H_2O_2 and 0.01 mM luminol, the potential range was set from −1.6 to +0.6 V.

Characterization. The stepwise reactions on the electrode surface were confirmed by electrochemical impedance spectroscopy (EIS). The semicircle portion observed at high frequencies corresponds to the electron-transfer limited process (R_{et}), and the linear portion observed at low frequencies by diffusion process.[5] As shown in Fig. S1A, the bare GCE revealed a small semicircle domain (curve a), which implied a low R_{et} value of the redox couple of $[Fe(CN)_6]^{3-/4-}$. Due to its nonconductive properties, CS film could inhibit the

electron transfer, leading to increased resistance for the redox probe (curve b). Upon immobilizing carboxylated GQDs (simply GQDs for short) on the CS modified electrode, R_{et} was remarkably increased (curve c), which implied that the carboxylated GQDs increased electron-transfer resistance due to the carboxylated GQDs carried more negative charges.[6] The R_{et} increased further after the assembly of peptide (curve d). After the phosphorylation of peptides by PKA and ATP-s, the resulting electrode showed a much higher resistance (curve e), indicating that phosphate groups had been transferred from ATP-s to peptides under the catalyzation of PKA. When capturing of Au NPs via Au-S bond on the modified electrode, the R_{et} decreased obviously (curve f), the reason can be attributed to that the assembled Au NPs on the electrode surface acted as electron transfer wire which accelerates the electron-transfer of $Fe(CN)_6^{3-/4-}$. To give more detailed information about the impedance of the modified electrode, a modified Randle-sequivalent circuit (inset in Fig. S1A) was chosen to fit the measured results. A cyclic voltammogram (CV) was also performed to characterize the assembly process of the modified electrode, and the results were well consistent with that of the EIS. As shown in Fig. S1B, a couple of quasi-reversible redox peaks of the probe were obtained on the bare GCE (curve a). The current decreased step by step with the assembly of CS, GQDs, peptide, and PKA-catalyzed phosphorylation (curves b–e), while the current increased obviously after the assembly of Au NPs via Au-S bond on the electrode surface (curve f). All these results demonstrate the sensing interface has been successfully fabricated.

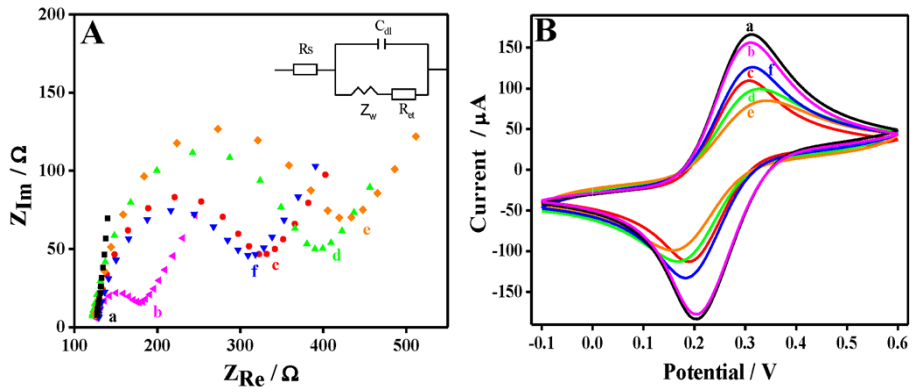

Fig. S1 (A) EIS and (B) CV of different modified electrodes in a 5 mM $[Fe(CN)_6]^{3-/4-}$ solution. (a) Bare electrode, (b) CS, (c) GQDs/CS, (d) peptide/GQDs/CS, (e) phosphorylated peptide/GQD/CS modified electrodes, and (f) electrode (e) after assembly of Au NPs. Inset: the equivalent circuit used to model the impedance data. Rs, Zw, and Cdl represent the solution resistance, the Warburg diffusion resistance, and the double-layer capacitance, respectively.

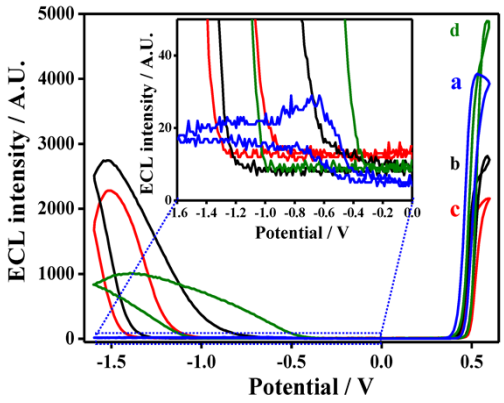

Fig. S2 ECL-potential curves of (a) bare electrode, (b) GQD/CS and (c) phosphorylated peptide/GQD/CS modified electrodes, and (d) electrode (c) after assembly of Au NPs in 0.1 M pH 7.4 PBS containing 0.01 mM luminol and 1.0 mM H_2O_2. Inset: the magnification of the ECL signal at potential range of 0 ~ -1.6 V.

The Possible Mechanism of the Dual-potential ECL Ratiometric Strategy. According to the mechanisms in the Fig. S3, we know that H_2O_2 was the coreactant to both the anodic ECL of luminol and the cathodic ECL of GQDs. From equation 1 to 4, we know that the luminol–H_2O_2 displayed a strong anodic ECL peak at about +0.55 V. In the presence of Au NPs as the catalyst, H_2O_2 might be broken up into $HO_2^{\bullet}$, further form the superoxide radical

anion ($O_2^{\bullet-}$). Then, luminol radicals react with $O_2^{\bullet-}$ to produce 3-aminophthalate anions which take place to strong light emission.[7] From equation 5 to 8, the cathodic ECL from GQDs was produced at about -1.25 V upon concomitant reduction of GQDs and H_2O_2. GQDs were reduced to $GQDs^{-\bullet}$ by charge injection upon the potential scan with an initial negative direction, while H_2O_2 was reduced to the strong oxidant hydroxyl radical ($OH^{\bullet}$); after that, $GQDs^{-\bullet}$ reacted with $OH^{\bullet}$ to emit light in the aqueous solution.[8] It is noted that Au NPs played an important role in the dual-potential ECL ratiometry strategy. On one hand, Au NPs served as the catalyst accelerating the oxidation of luminol on the electrode surface. On the other hand, the sufficient spectra overlap between the absorption band of Au NPs and the ECL emission band of GQDs makes the efficient ECL resonance energy transfer between Au NPs and GQDs possible. At higher kinase activity, more Au NPs would be captured onto the electrode surface, giving higher electrocatalytic efficiency to the luminol ECL reaction and better ECL resonance energy transfer with GQDs simultaneously. On the basis of the ratio of the enhanced anodic ECL from luminol to the quenched cathodic ECL from GQDs in one system, kinase activity can be determined indirectly. Moreover, the dual-potential ECL ratiometric strategy could decrease the background interference in complex samples by self-calibration of the two emission bands. Thus, the designed dual-potential ECL ratiometric approach can be used for kinase activity characterization accurately and sensitively.

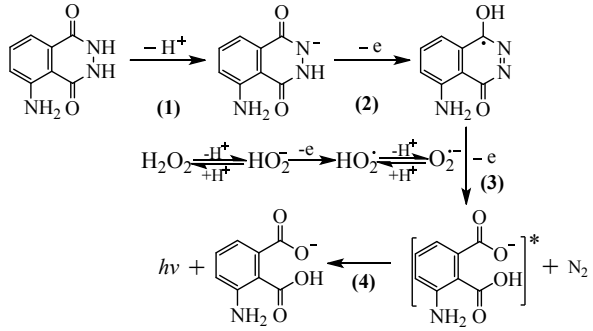

$$GQDs + e^- \longrightarrow GQDs^{\bullet -} \quad (5)$$

$$H_2O_2 + e^- \longrightarrow OH^{\bullet} + OH^- \quad (6)$$

$$OH^{\bullet} + GQDs^{\bullet -} \longrightarrow GQDs^* + OH^- \quad (7)$$

$$GQDs^* \longrightarrow GQDs + h\nu \quad (8)$$

Fig. S3 The possible mechanism of the dual-potential ECL ratiometric strategy.

Optimization of Detection Conditions. To efficiently apply the ECL ratiometric system to PKA detection, several experimental parameters including the concentration of peptide and the concentration of ATP-s were optimized (Fig. S4). The effect of peptide concentration on catalytic reaction was assessed by incubating variety concentrations of peptides (0–120 μM) with 0.1 U/mL PKA and 50 μM ATP-s in the reaction buffer containing other elements necessary to reaction. As shown in Fig. S4A, with increasing the concentration of peptide, the ECL intensity of luminol showed an initial quick increase followed by a slow enhancement of ECL intensity. However, the ECL intensity of GQDs showed an initial quick decrease followed by a slow reduction of ECL intensity. The logarithmic value of $ECL_{Luminol}/ECL_{GQDs}$ reached a maximal value at the peptide concentration of 100 μM and then leveled off. To obtain high sensitivity, the optimum peptide concentration should be 100 μM. As shown in Fig. S4B, the cathode ECL from GQDs decreased and the anode ECL from luminol increased correspondingly with increasing concentration ATP-s in the presence of 0.1 U/mL PKA. The logarithmic value of $ECL_{Luminol}/ECL_{GQDs}$ reached a maximal value at the ATP-s concentration of 50 μM and then leveled off. These results manifested that 50 μM ATP-s was sufficient to the phosphorylation reaction catalyzed by PKA.

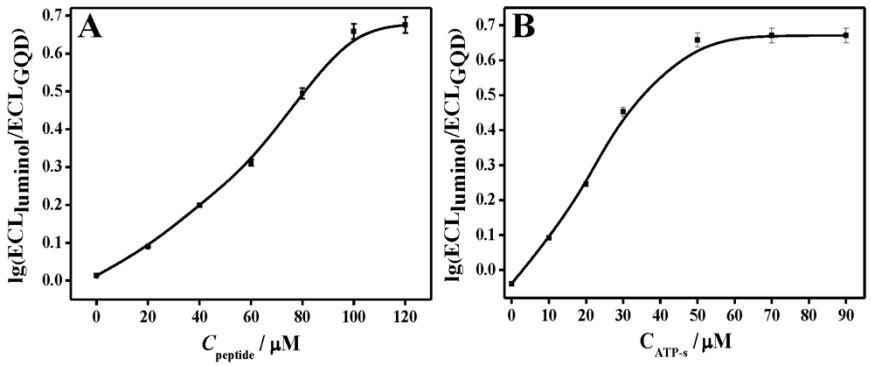

Fig. S4 Effect of concentration of (A) peptide and (B) ATP-s to the PKA detection.

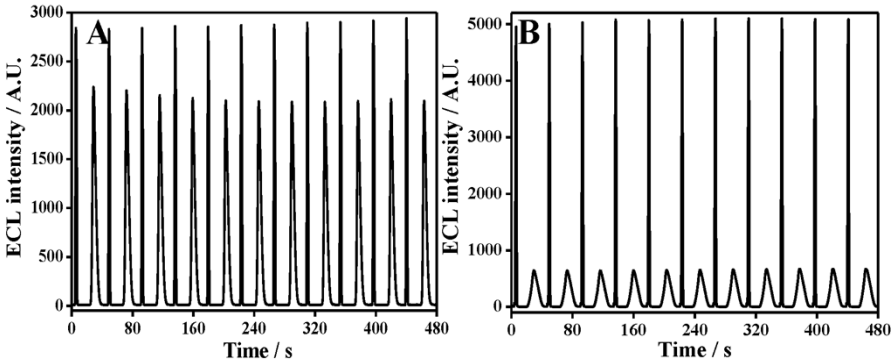

Fig. S5 ECL intensity-time curves of the biosensor at PKA concentration of (A) 0 U/mL and (B) 0.1 U/mL under continuous potential scan with a scan rate of 100 mV/s. Other conditions are the same as in Fig. 2.

Table S1 Comparison of different methods for PKA activity detection

Method	Linear range	Detection limit	Reference
ZrMMs-based flow cytometry	0.01−20 mU/μL	0.006 mU/μL	9
Ag nanoclusters-based fluorescence assay	0.001−2 U/μL	0.5 mU/μL	10
Synthetic phosphorylated receptor probe-based electrochemical assay	5−50 U/mL	0.1 U/mL	11
DNA-Au NPs network-based electrochemical assay	0.1−40 U/mL	0.03 U/mL	12
Upconversion nanophosphor-based luminescence resonance energy transfer assay	0.0001−0.01 U/μL	0.00005 U/μL	13
Peptide-templated gold nanocluster beacon-based fluorescence assay	0.001−4 U/mL	6 pM	14
TMSPs-based fluorescent assay	0.5−500 mU/μL	0.1 mU/μL	15
Ru(II) encapsulated phosphorylate-terminated silica nanoparticles-based ECL strategy	0.01−1 U/mL	0.005 U/mL	16
MB technology and GNP signal enhancement-based ECL assay	0.01−50 U/mL	0.005 U/mL	17
Gold nanoparticles amplification-based ECL assay	0.07−32 U/mL	0.07 U/mL	18
Semisynthetic GFP-based fluorescent assay	2.5−125 mU/μL	0.5 mU/μL	19
Dual-potential ECL ratiometric strategy	0.01−10 U/mL	0.005 U/mL	This work

Table S2 PKA activity measured in human serum with the as-proposed ECL assay

Samples	Add (U/mL)	Found (U/mL)	Recovery (%)
1	0.1	0.095	95
2	1.0	1.04	104
3	5.0	5.32	106

Detection of PKA Activity in Cell Lysates. Protein kinases have a significant impact on cell signaling, overexpression of protein kinase is generally associated with cell proliferation and neoplastic transformation. PKA is also served as a cancer biomarker for diagnostics and prognostics. Moreover, MCF-7 breast carcinoma cells expressed higher level of PKA than the other cell lines.[12] However, PKA in cell lysate without drug stimulation can be clearly detected with a relatively weak response, indicating a low level of PKA activity in cells.[9,12] To further testify the reliability of the dual-potential ECL ratiometric strategy, a series of samples were prepared by using 10 μg/mL cell lysate (without drug stimulation) spiked with different concentrations of PKA, and the correlation of the determination results for these samples by using the PKA ELISA Kit (Lanpai Bio.) and the proposed dual-potential ECL ratiometric strategy was investigated and the results of such comparative studies are shown in Fig. S6. It can be seen that a relatively good correlation is obtained between the two methods (R= 0.992), further demonstrating the reliability of the proposed method for PKA analysis in real samples.

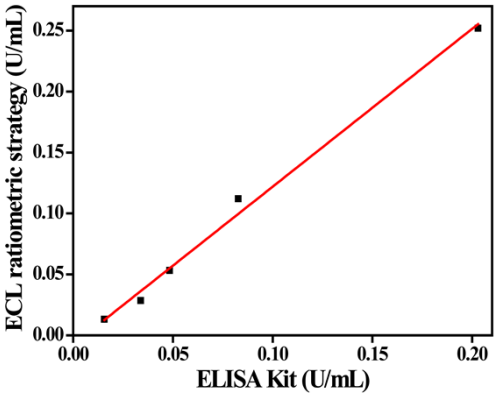

Fig. S6 Correlation of the ELISA Kit and ECL ratiometric strategy for the detection of PKA activity.

References

1 a) W. S. Hummers and R. E. Offeman, *J. Am. Chem. Soc.* 1958, **80**, 1339; b) N. I. Kovtyukhova, P. J. Ollivier, B. R. Martin, T. E. Mallouk, S. A. Chizhik, E. V. Buzaneva and A. D. Gorchinskiy, *Chem. Mater.* 1999, **11**, 771.

2 D. Y. Pan, J. C. Zhang, Z. Li and M. H. Wu, *Adv. Mater.* 2010, **22**, 734.

3 K. Yang, S. A. Zhang, G. X. Zhang, X. M. Sun, S. T. Lee and Z. Liu, *Nano Lett.* 2010, **10**, 3318.

4 a) K. C. Grabar, R. G. Freeman, M. B. Hommer and M. J. Natan, *Anal. Chem.* 1995, **67**, 735; b) R. P. Liang, Z. X. Wang, L. Zhang and J. D. Qiu, *Chem-Eur. J.* 2013, **19**, 5029.

5 S.-M. Park and J.-S. Yoo, *Anal. Chem.,* 2003, **75**, 455A.

6 E. Han, L. Ding, H. Lian and H. Ju, *Chem. Commun.,* 2010, **46**, 5446.

7 S. Xu, Y. Liu, T. Wang and J. Li, *Anal. Chem.* 2010, **82**, 9566.

8 P. Wu, X. Hou, J. Xu and H. Chen, *Chem. Rev.* 2014, **114**, 11027.

9 W. Ren, C. Liu, S. Lian and Z. Li, *Anal. Chem.* 2013**, 85**, 10956.

10 C. Shen, X. Xia, S. Hu, M. Yang and J. Wang, *Anal. Chem.* 2015, **87**, 693.

11 I.-S. Shin, R. Chand, S. W. Lee, H.-W. Rhee, Y.-S. Kim and J.-I. Hong, *Anal. Chem.* 2014**, 86**, 10992.

12 Z. Wang, N. Sun, Y. He, Y. Liu and J. Li, *Anal. Chem.* 2014**, 86**, 6153.

13 C. Liu, L. Chang, H. Wang, J. Bai, W. Ren and Z. Li, *Anal. Chem.* 2014**, 86**, 6095.

14 Q. Wen, Y. Gu, L.-J. Tang, R.-Q. Yu and J.-H. Jiang, *Anal. Chem.* 2013**, 85**, 11681.

15 J. Bai, Y. Zhao, Z. Wang, C. Liu, Y. Wang and Z. Li, *Anal. Chem.* 2013**, 85**, 4813.

16 Z. Chen, X. He, Y. Wang, K. Wang, Y. Du and G. Yan, *Biosens. Bioelectron.* 2013**, 41**, 519.

17 Z. Zhao, X. Zhou and D. Xing, *Biosens. Bioelectron.* 2012**, 31**, 299.

18 S. Xu, Y. Liu, T. Wang and J. Li, *Anal. Chem.* 2010**, 82**, 9566.

19 C. Yin, M. Wang, C. Lei, Z. Wang, P. Li, Y. Li, W. Li, Y. Huang, Z. Nie and S. Yao, *Anal. Chem.* 2015**, 87**, 9566.